Parametrization of the Low Energy Cross Sections for $\gamma He^3 \dashrightarrow pd$

Kirk McDonald

Revised July 7, 1970

To parameterize the angular distribution of $\gamma He^3 \dashrightarrow pd$, we use a multipole analysis, but consider only relative S, P, and D waves for the pd state. (A detailed computation of the multipoles keeping only S and P waves is given by Abe Seiden in CTSL Internal Report No. 49) The multipoles of interest are the electric dipole (E1), magnetic dipole (M1), and the electric quadrupole (E2). The possible couplings between the various multipoles and pd states are listed below.

E1 $\dashrightarrow$	M1 $\dashrightarrow$	E2 $\dashrightarrow$
$^2P_{1/2}$	$^2S_{1/2}$	$^4S_{3/2}$
$^2P_{3/2}$	$^4S_{3/2}$	$^2D_{3/2}$
$^4P_{1/2}$	$^2D_{3/2}$	$^2D_{5/2}$
$^4P_{3/2}$	$^4D_{1/2}$	$^4D_{3/2}$
	$^4D_{3/2}$	$^4D_{5/2}$

For photon energies small compared to the nucleon mass only a few of these possible amplitudes are expected to dominate. M1 and E2 amplitudes are roughly equal in strength and both weaker than the E1. The M1 amplitudes couple much more strongly to spin than orbital angular momentum, so that if we assume the He^3 is in a $^2S_{1/2}$ state, the most important M1 transition is to the $^4S_{3/2}$ pd state. Conversely, in the low energy limit, electric transitions couple more strongly to orbital angular momentum than to spin, and this coupling is independent of the total angular momentum. Hence we expect E1 transitions to $^2P_{1/2}$ and $^2P_{3/2}$ to dominate and be roughly equal, while for E2 transitions we need only consider the $^2D_{3/2}$ and $^2D_{5/2}$. For simplicity, denote these five amplitudes as S_3, P_1, P_3, D_3 and D_5.

Keeping only these five amplitudes, the differential cross-section has the form

$A + B\cos\theta + C\sin^2\theta + D\sin^2\theta\cos\theta + E\sin^2\theta\cos^2\theta \qquad (\theta = \theta_{c.m.})$

If we assume that $P_1 = P_3$ and call their common value P, and that $D_3 = D_5$ and call their common value D/5, then

$A = S_3^2 \quad B = 0 \quad C = 3P^2 \quad D = 2\sqrt{6}\mathrm{Re}P^*D \quad E = 2D^2$

If these assumptions hold, the phase, ϕ, between P and D is given by

$$\cos\phi = \sqrt{EC}/2D$$

This form of the multipole analysis is used by nuclear physicists dealing with photon energies less than 50 MeV. In particular see

Bailey, Griffiths, and Donnelly, Nuc. Phys. A94, 502 (1967)

If we keep all five amplitudes then

$A = S_3^2 + (2/3)(P_3 - P_1)^2 + 4(D_3 - D_5)^2$

$B = 4\sqrt{2/3}\mathrm{Re}(P_1 - P_3)^*(D_3 - D_5)$

$C + P_3^2 + 2\mathrm{Re}P_3^*P_1 - 2(D_3 - D_5)^2$

$D = 2\sqrt{2/3}(5\mathrm{Re}P_1^*D_5 + 2\mathrm{Re}P_3^*(3D_3 + 2D_5))$

$E = 5(3D_5^2 - D_3^2 + 8\mathrm{Re}D_3^*D_5)$

I have located three experiments giving differential cross-sections for $\gamma He^3 \dashrightarrow pd$ in the vicinity of $E_\gamma = 100$ MeV.:

1. Fetisov et al, Nuc. Phys. 71, 305 (1965) A Bremsstrahlung weighted average for $22 < E_\gamma < 170$ MeV.
2. Bachelier et al, Phys. Letters 21, 697 (1966) Actually $pd \dashrightarrow He^3\gamma$ with $T_p = 156$ MeV.
3. Carron, Phys. Rev. 168, 1095 (1968) Refers to unpublished data by O'Fallon et al. at $E_\gamma = 60$ MeV.

The figures show these cross-sections.

For purposes of calculation, I normalised the data to 1.0 at 90°, and combined all three experiments. Thus A + C should be 1.0. The results of a least squares fit are

	A	B	C	D	E	ϕ
My fit	0.39	-0.024	0.60	1.33	0.99	$\pm 73^\circ$
Bailey et al E_γ = 40 MeV.	.0006	-	1.0	1.30	0.48	$\pm 74^\circ$

Since $\cos\phi = .3$, the smallnes of B compared to D implies either $P_1 = P_3$ or $D_3 = D_5$, or both, even near E_γ = 100 MeV. The increase in A means either S_3 in increasing or P_1 no longer equals P_3 etc. Note that a rise in A and a fall in C is consistent with a phase difference between P_1 and P_3 or a phase difference between D_3 and D_5. The increase in E can only come from an increase in the D wave amplitudes, and a phase difference between D_3 and D_5 would slow the increase, so I surmise $D_3 = D_5$ still, so that $P_3 \neq P_1$ any more. The constancy of coefficient D most likely implies that either P_3 is decreasing or the P_3-D_{3or5} phase difference is closer to 90°.

A more or less consistent solution to Bailey's paramters is

$S_3 = 0 \quad P_1 = P_3 = .6 \quad D_3 = D_5 = .1 \quad \phi_P = 74^\circ$ defining $\phi_D = 0^\circ$

Supposing the magnitude of the P waves remain constant, my fit implies

$S_3 = .5 \quad D_3 = D_5 = .14 \quad \phi_{P_1} = 35^\circ \quad \phi_{P_3} = 105^\circ$ with $\phi_D = 0^\circ$

The large size of S_3 probably implies that the assumption about the magnitudes isn't valid. However, a large S_3 term would be nice in that it is the only one of the amplitudes which can interfere with a $\Delta(1236)$ intermediate state.

It is clear from fig. 2 that the effective cross section of the $He^3(\gamma, p)D^2$ reaction has a wide maximum at photon energies $\approx$ 12 to 13 MeV. The effective cross section at the maximum is $\approx$ 1.0 mb.

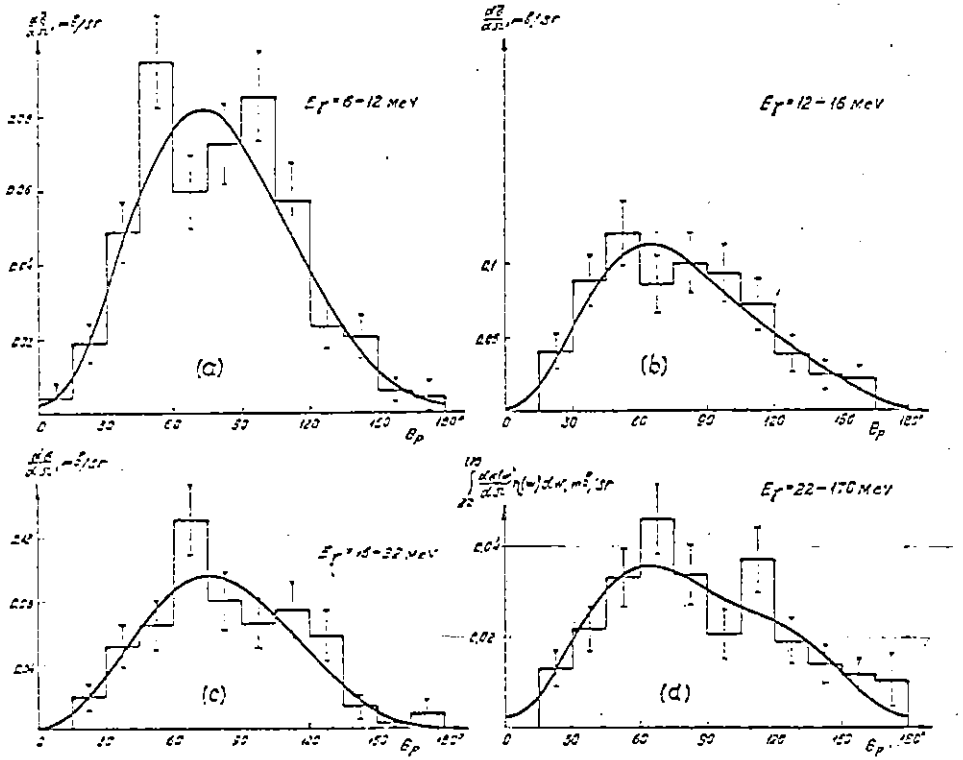

Fig. 3. Angular distributions of protons in the $He^3(\gamma, p)D^2$ reaction in the c.m. system.

3.2.2. *Angular distribution of protons.* The angular distributions of protons emitted in the $He^3(\gamma, p)D^2$ reaction are given in fig. 3 in the c.m. system for several γ-quantum energy intervals. The proton emission angle in the c.m. system is plotted in abscissa versus the cross section $d\sigma/d\Omega$ averaged over the energy interval in mb/sr. The smooth curve in the plot is calculated by the least squares method in the form

$$f(\theta) = A(\sin^2\theta + \beta\sin^2\theta\cos\theta + \gamma\sin^2\theta\cos^2\theta + \delta). \quad (7)$$

The coefficients A, β, γ and δ are given in table 1. It is clear from table 1 and fig. 3 that at photon energies below 22 MeV the isotropic component of the angular distributions of protons is very small. At high energies the isotropic part increases appreciably. The asymmetry of the angular distributions shifting the maximum forward appears near the threshold of the reaction, reaches its maximum at photon energies of 12 to 16 MeV and then gradually decreases. The coefficient γ tends to increase as the photon energy increases.

TABLE 1

Coefficients A, β, γ and δ characterizing the angular distribution of protons in the $He^3(\gamma, p)D^2$ reaction

Energy interval E_γ (MeV)	6-12	12-16	16-22	22-170	6-22	6-170
A (mb/sr)	0.072±0.065	0.086±0.013	0.091±0.011	0.028±0.004	0.123±0.008	0.153±0.00
β	0.69 ±0.14	0.95 ±0.25	0.57 ±0.18	0.57 ±0.24	0.7 ±0.1	0.66 ±0.1
γ	0.1 ±0.3	0.9 ±0.6	0.1 ±0.4	1.1 ±0.6	0.4 ±0.2	0.5 ±0.2
δ	0.03 ±0.04	0.02 ±0.08	0.02 ±0.06	0.09 ±0.11	0.01 ±0.02	0.03 ±0.02
$\sigma = \sigma(\frac{8}{3}\pi A)$	1.06 ±0.09	1.21 ±0.17	1.05 ±0.12	1.35 ±0.20	1.09 ±0.05	1.14 ±0.05

3.3. THREE-PARTICLE DISINTEGRATION (REACTION $He^3(\gamma, n)2p$)

3.3.1. *Effective cross section.* The effective cross section of the $He^3(\gamma, n)2p$ reaction determined from 515 measurements of this reaction is given in fig. 4. The histogram shows the average effective cross section in each photon energy interval. To make the comparison with theoretical predictions more convenient the histogram is approximated over the area by a smooth curve. It is clear from fig. 4 that the effective cross section has a very wide maximum at photon energies between 16 and 19 MeV, the cross section at the maximum being $\approx$ 1.0 mb just as for the two-particle channel.

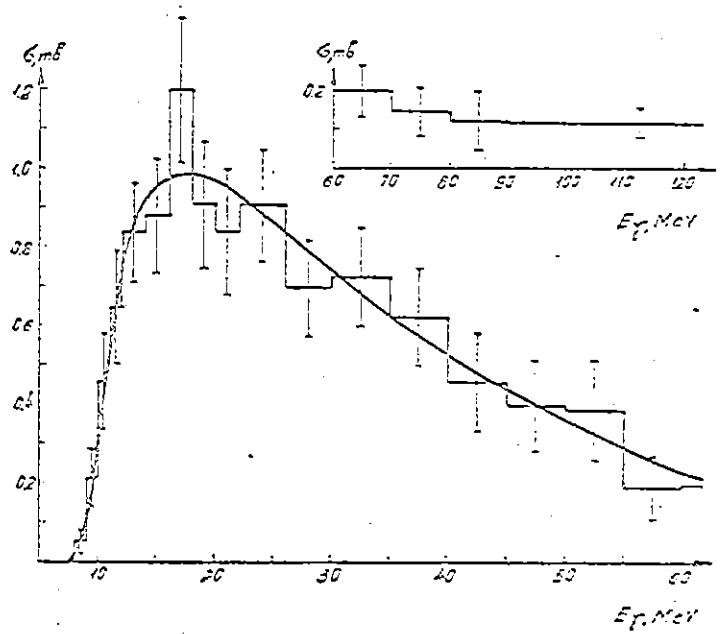

Fig. 4. Effective cross section of the $He^3(\gamma, n)2p$ reaction.

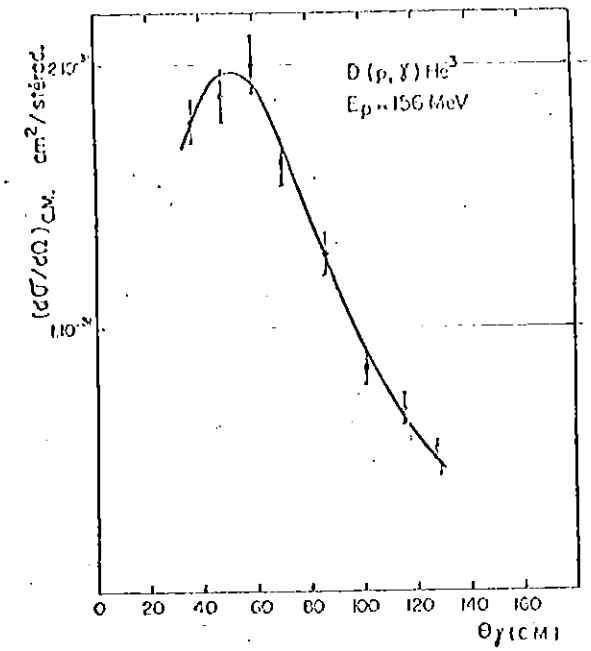

Fig. 2. Section efficace différentielle de la réaction $D(p,\gamma)^3He$ à E_p = 156 MeV, dans le système du centre de masse.

leur temps de vol entre la cible et les détecteurs, enfin avec une moindre précision par l'énergie des photons. Chaque évènement est donc largement surdéterminé.

Le faisceau externe de protons du synchrocyclotron d'Orsay frappe une cible de polyéthylène deutéré (18 mg/cm^2) placée au centre de la chambre à réaction. Les photons sont détectés par un compteur Čerenkov à absorption totale constitué par un bloc de verre au plomb de 20 cm d'épaisseur associé à un photomultiplicateur rapide 60 A. V. P.; le compteur présente l'intérêt de ne donner aucun effet direct pour les nombreuses particules lourdes reçues. L'angle solide Ω_γ est défini par un canaliseur de plomb (de 6 cm d'épaisseur).

Les noyaux ^3He sont détectés par deux scintillateurs minces en coïncidence formant télescope et placés au voisinage du plan focal de l'analyseur magnétique. Les diaphragmes d'entrée de ce dernier sont ouverts de manière à admettre sans perte appréciable tous les noyaux de recul ^3He (> ~98%) associés aux photons de la réaction reçus dans l'angle solide Ω_γ. Le dispositif électronique utilisé comporte sur la voie γ une porte linéaire rapide suivie d'un allongeur et d'un analyseur multicanal à aiguillage réglé sur deux voies. La porte est ouverte par l'un ou l'autre de deux circuits de coïncidence de temps de résolution voisin (~2×10^{-8} s), permettant, par un réglage convenable des retards, d'obtenir parallèlement le spectre γ en coïncidence avec les noyaux de ^3He et un spectre de fortuites.

On a représenté fig. 1a des spectres obtenus à $\theta_\gamma = 50°$. Le spectre γ "vrai" comporte une raie de largeur instrumentale voisine de 40 MeV correspondant aux photons de la réaction cherchée, toutes les conditions cinématiques étant respectées. Dans le cas contraire, on retrouve un spectre rapidement décroissant analogue au spectre "fortuit". La contribution de ce dernier est d'ailleurs presque toujours négligeable dans la région de la raie. Le résidu de coïncidences vraies observé pour les petites impulsions est dû aux effets de bord du canaliseur. Les figs. 1b et 1c représentent des raies obtenues par analyse magnétique des noyaux de ^3He en coïncidence avec les photons. Pour les différentes valeurs de θ_γ, ces raies sont centrées sur les valeurs attendues et leurs largeurs s'interprètent bien, compte tenu du ralentissement de ^3He dans la cible, de l'ouverture angulaire du compteur γ dans le plan de réaction et de la largeur du détecteur. En général, les mesures ont été effectuées pour une série de valeurs de la fréquence de la sonde de mesure de champ correspondant à des bandes d'analyse juxtaposées, de telle manière que le nombre total d'évènements cherchés soit simplement la somme des évènements enregistrés dans chaque bande (après normalisation au même nombre de protons reçus par la cible). Il suffisait ainsi dans la pratique de 4 à 6 mesures pour enregistrer la totalité de la raie.

Nous avons porté sur la fig. 2 les sections efficaces différentielles $(d\sigma/d\Omega)_{\theta_\gamma}$ dans le système du centre de masse, déduites de ces mesures. Les erreurs indiquées sont les erreurs statistiques. On peut estimer à 20% l'ordre de grandeur d'une erreur systématique éventuelle sur l'ensemble de la courbe, provenant en particulier de l'évaluation de l'angle solide moyen du détecteur γ, de celle du nombre d'atomes de deutérium dans la cible, ou d'un défaut d'étalonnage de la chambre d'ionisation à hélium utilisée comme moniteur du faisceau.

La section efficace totale de la réaction a été calculée par intégration à partir des résultats ci-dessus, en ajoutant une correction de 15% estimée par extrapolation, pour tenir compte de la contribution des petits et des grands angles. La valeur obtenue est de 1.4 ± 0.3 μb; les mesures de Fetisov et al. [3] pour la réaction de photodésintégration inverse peu précises dans le domaine d'énergie des photons supérieur à

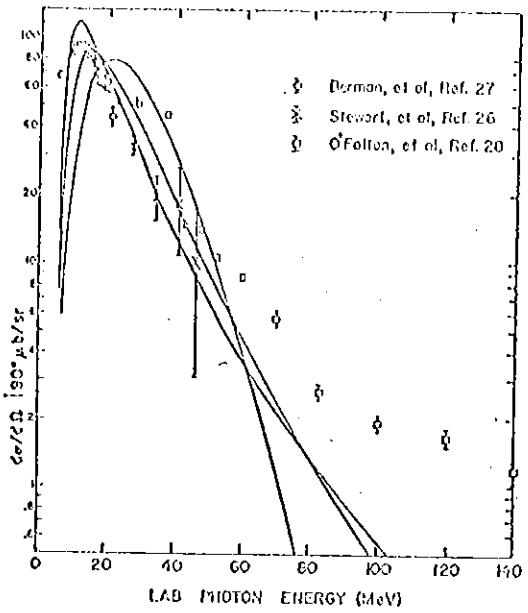

FIG. 4. Ninety degree differential cross section for the E·r interaction. Curve (a), Gaussian, $\mu^{-1}=4.1$; (b) Ψ_3, $\mu_1^{-1}=1.9$, $\mu_2=1.44\mu_1$; (c) Gunn-Irving, $\mu^{-1}=2.6$. Experimental points are from Refs. 26, 27, and 28.

20% too high. The fact that the 90° results are much too small at high energies whereas the total cross section remains quite good is due to the forward peaking of the angular distribution, as shown in Fig. 5 at 60 MeV (curves 1 and 2). It practically disappears in the backward hemisphere and the peaking at 45° is greatly pronounced, in disagreement with experiment.

Also shown in Fig. 5 are the angular distributions for ψ_2 and ψ_3 using Foldy's interaction $\int_0^1 ds\, e^{isk\cdot r}$ (curves 1′ and 2′), which gives a result intermediate between the dipole distribution ($\sin^2\theta$ in the center of mass) and the E·r results with the full retardation factor. This improves the angular distribution greatly but it is still too small in the backward hemisphere.

We also show in Fig. 5 the distribution from the A·p interaction (curve 3) for the Gunn-Irving wave function. For ease in comparison we have multiplied the actual theoretical result by 3.38 to normalize the curve to the 60° data point. The angular distribution is not greatly different from that of the Foldy interaction, but it is even smaller for large angles.

This fact, that the differential cross section agrees so poorly, indicates that we cannot take too seriously the agreement of the total cross at high energy. That a singular wave function which ignores mesons and produces an incorrect differential cross section should yield the correct total cross section at high energies must be regarded as somewhat fortuitous.

Of course the differential cross section is much more sensitive to the details of the wave function than is the total cross section. It would be very surprising if such a simple model as we are using were to correctly describe the details of the nucleus at an interaction energy of say 60 MeV or greater, where short wavelengths begin to probe the internal structure. This means that the differential cross section at low or intermediate energies ($\lesssim$50 MeV) is a sensitive test of the ground-state wave function. It is at the intermediate energies that various models will differ in their predictions sufficiently enough to be able to derive meaningful information from comparison with experiment. Accurate experimental differential cross sections in this energy range would be very helpful.

As mentioned in the Introduction, the final deuteron should have a radius which is smaller when the free proton is near and larger when farther away. Since our deuteron is more spread out than the helium, this correction would have the effect of increasing the overlap of the initial and final states, thereby increasing the cross section.

To qualitatively investigate the effect of a final-state interaction we have inserted a proton-deuteron square-well attraction of depth 75 MeV and radius 1.5 F. This increases the peak cross section by about 15% and decreases the high-energy ($\gtrsim$35 MeV) cross section by nearly a factor of 2. The result is quite sensitive to the potential radius. The same low-energy effect has been noticed by Eichmann.[4]

These last results are encouraging, for they tend to bring the nonsingular wave function Ψ_3 into better agreement with the low-energy data. In fact, they will also tend to bring the A·p results into better agreement, although it is very doubtful that final-state interactions could account for nearly a factor of 2. The large difference between the two interactions is most likely due to the use of inexact wave functions.

We finally see that the three wave functions tried cannot match both the photodisintegration cross sec-

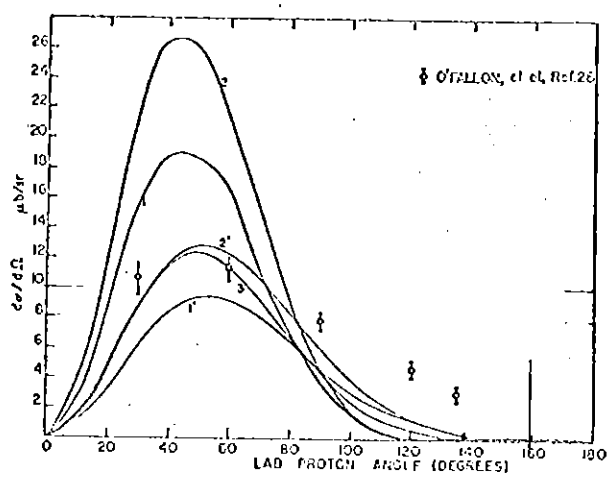

FIG. 5. Angular distribution at 60 MeV for three different interactions. Curves 1, 1′, and 3 are the Gunn-Irving wave function Ψ_3 with $\mu^{-1}=2.6$F. Curves 2 and 2′ are Ψ_3 with $\mu_1^{-1}=1.9$F., $\mu_2=1.44\mu_1$. Curves 1 and 2 are the interaction E·r with the full retardation factor $e^{ik\cdot r}$. Curves 1′ and 2′ are the E·r interaction with the Foldy space dependence $\int_0^1 ds\, e^{isk\cdot r}$ for the electric field. Curve 3 is the A·p interaction multiplied by 3.38 to normalize to the 60° data point. Experimental points are from Ref. 28.

Figure 5. The O'Fallon data for $\gamma He^3 \longrightarrow pd$.